Journal of Materials Science and Surface Engineering, 11: 1112-1117
ISSN (Online): 2348-8956; DOI: https://doi.org/10.52687/2348-8956/1101

Peer Reviewed

Structural, Optical and Electrical Study of Tin Sulphide (SnS) Nanostructure Thin Films Synthesized via Electrodeposition Technique

Nathu Lal[1,3] · Madhu Yadav[2] · Kanhaiya Chawla[1,4] · Sandeep Sharma[1,5] · Chhagan Lal[1,2]

[1] Department of Physics, University of Rajasthan, Jaipur, Rajasthan 302004, India.
[2] Centre for Non-Conventional Energy Resources, University of Rajasthan, Jaipur, Rajasthan 302004, India.
[3] Govt. Girls College, Jhunjhunu, Rajasthan 333001, India.
[4] Govt. College, Pratapgarh, Rajasthan 312605, India.
[5] Govt. College, Jhunjhunu, Rajasthan 333001, India.

ABSTRACT

In current study tin sulphide (SnS) nanostructure thin films were grown successfully on ITO substrate by electrodeposition method. The structural and morphological properties of deposited nanostructures were examined by XRD and SEM. X-ray diffraction analysis informed about orthorhombic crystal structure and the calculated crystal size was approximately 48 nm for preferred orientation. The optical properties were examined by UV-visible absorbance spectra and optical band gap was measured using Tauc plot. The deposited SnS nanostructure has a direct band gap ~1.31eV at room temperature. Additional characteristics like superior optical transmission and low electrical resistance were also the subject of investigations. The band gap energy is lower than that of bulk material because the formed nanostructure contains defect states. The current-voltage characteristics were measured in the dark and with tungsten filament light (100 W) and LED illumination, respectively. Compared to dark mode, there was noticeable variation in the current for both conventional light and LED. Last but not least, based on the academic knowledge already available, including recent scientific advancements, the obstacles and potential for future research on SnS compounds are emphasized.

ARTICLE HISTORY
Received 28-07-2023
Revised 20-12-2023
Accepted 22-12-2023
Published 04-04-2024

KEYWORDS
Nanostructure
Electrodeposition
Optical Properties
Electrical Resistivity
Illumination

Introduction

Emerging materials research and studies have concentrated on the simple and cost-effective design and manufacture of nanostructure with regulated size and form, which is technologically relevant. Due to the unique electrical and physiochemical properties, semiconductor, and metal oxide/sulphide nanostructures such as nano particles, nanorods, nanotubes, nanowires, nanoplates, and nanoflowers have attracted a lot of attention [1,2]. Due to their advantageous features and ease of production, binary and ternary materials such as GaAs, Cu (In,Ga)$(S,Se)_2$ (CIGS) solar cells, $Zn_{1-x}Ge_xO$ and others have opened different routes as contrast to silicon-dependent technology. Numerous novel and cutting-edge materials have been suggested as suitable components for solar cells over the past few years. To lower the cost of the solar cell overall by increasing the photovoltaic conversion efficiency, research is being done to take use of their features either as individual thin films or when used in a device. For thin film photovoltaic (PV) technology to become a significant energy source, cost-efficient, long-lasting, and carbon neutral absorber materials are needed. According to research, photovoltaic (PV) and photoelectrochemical (PEC) devices can use thin-film materials to convert solar energy. Due to the various potential applications, a number of efforts have been used to create and characterise various metal chalcogenides and inorganic materials to increase their efficiency in many applications. The electrical, structural, and optical features of nanostructured metal sulphides make them favourable materials for use in energy, biomedicine, and optoelectronics, among other applications. However, the development of photovoltaic thin films is hampered by the hazardous "heavy metals" Cd and Se as well as the high cost of the elements In and Ga [3-6]. One of the IV-VI group-belonging compounds is tin mono sulphide (SnS) which is p-type semiconductor material. SnS has a high absorption coefficient of $\sim 10^5$ cm^{-1} [4] therefore got special interest since it is a low-toxic photoconductor that can be used to make NIR detector materials and photoelectric energy conversion equipment. Sn and S, the components that make up the substance, are abundant and less hazardous. Depending on the deposition method and measuring technique used, the optical band gap for SnS films ranges from 1.0 to 1.5 eV [1,7-8]. For single junction solar cells, this bandgap energy sequence follows the Shockley-Queisser Efficiency Limit [9]. The SnS phase may be accompanied by additional complexes primarily made of SnS_2, Sn_2S_3, and Sn_3S_4 depending on the manufacturing temperature and concentration of constituent, but technologically the most stable substances are SnS and SnS_2 compounds. In order to create a two-layered structure with a wide interlayer separation, the Sn and S atoms are strongly linked. The SnS has an orthorhombic layered crystal structure with lattice values of a=0.4329, b=1.1193 and c=0.398 nm [10]. When black phosphorus (BP) was initially exfoliated into a monolayer form in 2014, it has made significant progress. One of the most widely used black phosphorus analogues (BPAs), SnS, shares the same ground-state orthorhombic structure as BP and has excellent potential in a wide range of fields due to its high mobility, moderate thickness-dependent bandgap, and

Corresponding Author: Nathu Lal, Tel: *+919887604347*
Email: gudha.phy@gmail.com
Contents lists available at http://www.jmsse.in/ & http://www.jmsse.org/

anisotropic electrical and thermal conductivity, among other properties while the bulk SnS shows indirect bandgap [11-13]. Ghosh et al. reported that the Sn-to-S ratio alters the energy band structure of SnS as well as the valence band and conduction band density states [14].

SnS nanostructures may be produced using a variety of fabrication techniques such as thermal evaporation [15], pulsed laser ablation [16], spray pyrolysis technique [17,18], DC magnetron sputtering [19], sol-gel spin coating [20], chemical bath deposition [21], successive ionic layer absorption and reaction [4], Atomic Layer Deposition [22], sputtering method [23] and electrodeposition [1,7,8,24]. This study includes preparation of nanostructure thin films of tin sulphide (SnS) on ITO substrates by a low-cost two electrode electrodeposition approach at constant potential.

Experimental

Materials and method

The SnS nanostructure thin film was grown using a traditional homemade two electrode electrochemical bath. We employed an ITO coated glass substrate as the working electrode and a graphite sheet as the counter electrode. Both electrodes were introduced in the solution through two steel tubes. The electrolyte solution was prepared by stannous (tin) sulphate $SnSO_4$ and sodium thiosulphate $Na_2S_2O_3.5H_2O$ of 0.05 M and 0.1 M concentration respectively. The pH value of solution was adjusted to 1.92 by adding few drops of dilute H_2SO_4 in prepared solutions and stirred on magnetic stirrer for 30 to 40 minutes at room temperature. Before starting the deposition procedure, the ITO glass substrate was cleaned using an ultrasonication method with acetone and rinsed with ultrapure water to eliminate impurities. A thin layer of SnS nanostructures was deposited on ITO sheet using HTC power supply DC 3002 at potential difference of 2.5 V for 30 minutes. The deposited sample was heated about 40° C for 10 minutes for dehydration or to remove any surface impurities then the temperature gradually decreases. It is predicted that the growth of SnS nanostructure on the ITO-coated glass sheet will react similarly to the deposition of other sulphide semiconductors. It was clear that $Na_2S_2O_3$ is unstable, and sulphur can be easily separated from it in an acidic solution [25]. The possible chemical reactions for deposition of SnS nanostructure thin film using aquas medium of stannous (tin) sulphate salt with sodium thiosulphate.

$$S_2O_3^{2-} + 2H^+ \rightarrow S + H_2SO_3 \qquad \text{(i)}$$

$$Sn^{2+} + S + 2e- \rightarrow SnS \qquad \text{(ii)}$$

Characterization of the nanostructure

Using Siemens D-5000 X-ray diffractometer with Cu Kα [λ=1.54Å] radiation, X-ray diffraction (XRD) was used to examine the structural characterization of the synthesized SnS nano structure thin films. SEM connected to EDX was used to analysis the surface morphology and microstructure with elemental mapping of the deposited nanostructures. (Model: JSM-7610F Plus & make: JEOL). Shimadzu UV-2600 UV-visible Spectrometer was used to analyse the optical characteristics and Fourier Transform Infrared Spectrometer (FTIR) Bruker Alpha was used to collect data on bonding in the range of 4000–500 cm^{-1}. The electrical properties (such as *I-V* characteristics) were measured by Keithley Electrometer 6517A.

Results and Discussion

Structural Analysis

Figure 1 shows the XRD diffractograms of the deposited SnS nanostructure with an angular scanning range of (10° – 70°) which explore the nature of the material, purity, and crystal structure. The sharp peaks in obtained spectrum correspond to the (110), (111) and (112) planes, which are related to orthorhombic layered crystal structure of deposited SnS nanostructure. The noticeable sharp peaks show that the synthesized nanostructure has a good crystalline character. The Debye-Scherrer equation was used to compute the crystallite size D (nm) [24,25].

$$D=\frac{0.9\lambda}{\beta \cos\theta} \qquad \text{(iii)}$$

where λ=1.54 Å is the wavelength of the incident X-ray radiation (Cu Kα), β is the full width at half maximum (FWHM) in radian, and 2θ is the Bragg's diffraction angle in radian of the preferred orientation. The mean crystalline size (D) calculated using equation (iii) for the deposited nanostructure was found 47.92 nm at preferred orientation. Patel et al. 2013 reported that the SnS nanostructures can have larger crystallites and better crystal quality at temperature in the range 300-500° C. It has also been observed that growing the crystallite size of SnS structures by raising the annealing temperature can result in the creation of larger grains [26].

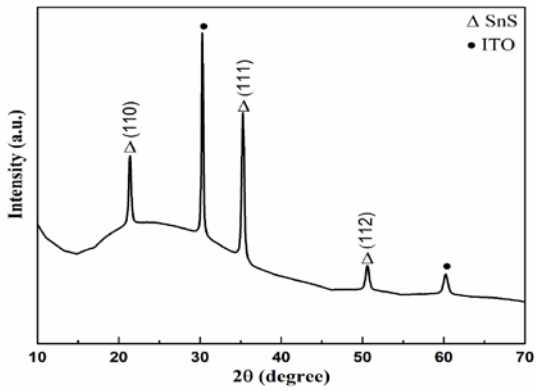

Figure 1: XRD spectrum of synthesized SnS nanostructure thin films

UV-Visible Analysis

The absorbance and transmittance spectra of the deposited SnS nanostructure thin films were obtained in the range of 300 to 800 nm which were shown in Fig. 2 (a) and (c) respectively. The deposited nanostructure thin films have a strong absorbance in the visible wavelength region. The plot of $(\alpha h\nu)^2$ *vs* photon energy also obtained and shown in Fig. 2(b). It has been observed that the curve is linear over a wide range of photon energies, which indicates the direct type of transitions in the SnS nanostructure. The optical band gap was determined using Tauc's formula [27].

$$(\alpha h\nu)^2 = C(h\nu - E_g) \qquad \text{(iv)}$$

where α is the absorption coefficient, h is the Plank's constant, ν is the frequency of incident photon, C is a constant and E_g is the direct transition band gap. The value of optical band gap was determined from the intersection of the extrapolation of the linear part and the horizontal axis 1.31 eV by extrapolating the linear portion of the plot $(\alpha h\nu)^2$ vs $h\nu$ as shown in inset Fig. (2b). As a result, nano

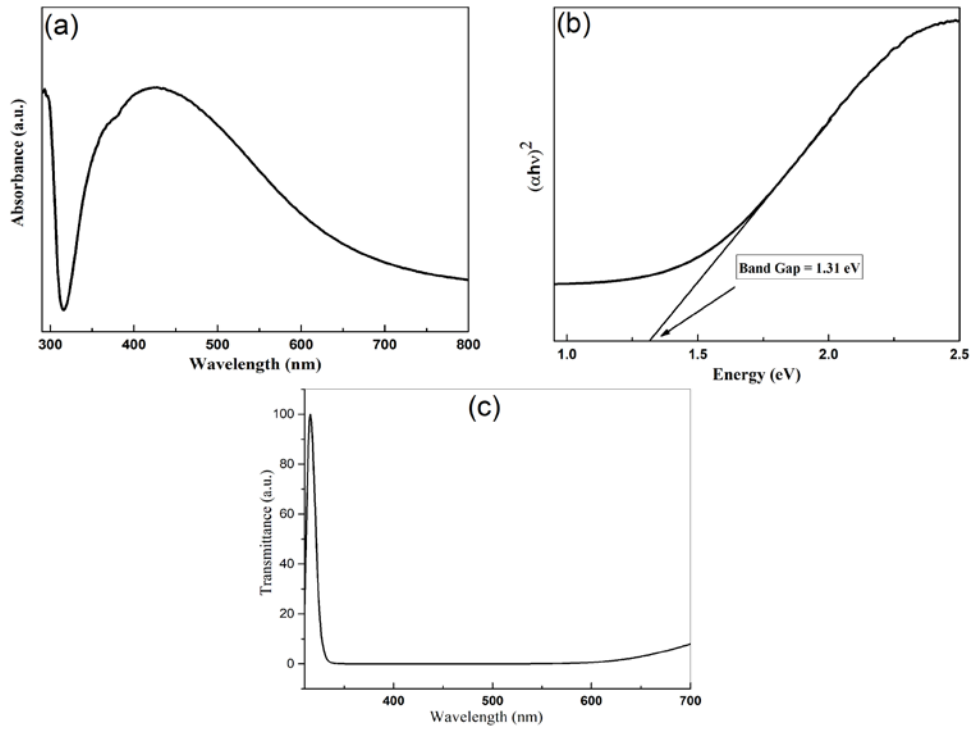

Figure 2: UV-visible spectra of synthesized SnS nanostructure. (a) absorbance spectrum (b) Tauc's plot (c) Transmittance spectrum

SnS-structure has strong visible absorption and optical band gaps close to ideal direct inter-band edges can be good candidates for the creation of hetero-junction solar cells' effective absorber layer. According to the quantum confinement effect, the bandgap energy rapidly increases as the SnS thickness decreases. When the thickness of the SnS thin film decreased, the absorption property showed a trend of a blue shift in the absorption edge [28]. Defect states induce the band gap of metal oxide nanostructures to decrease, hence the significant variation in band gap energy is caused by these defect states. Both nanoparticles and nanostructures show the same trend in band gap energy fluctuation; but, due to greater lattice strain and a higher surface to volume ratio, nanostructures have a lower band gap energy than nanoparticles of the same size [29].

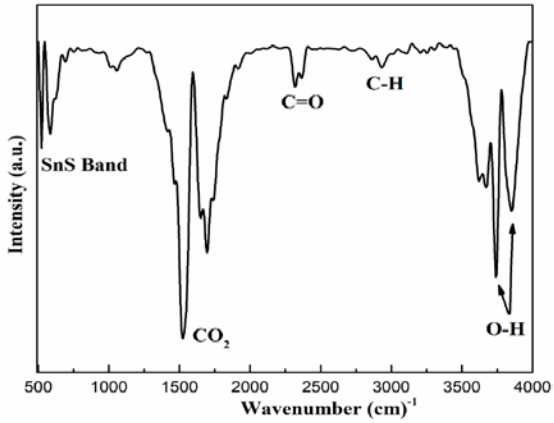

Figure 3: FTIR spectrum of synthesized SnS nanostructure

FTIR Analysis

FTIR spectroscopy was used to identify the organic or inorganic substances contained in the nanostructure sample which are associated to various functional groups. The FTIR spectra of SnS nanostructure thin film was obtained in the range of 500 - 4000 cm^{-1} and shown in Fig. 3. The prominent peak that can be noticed below 750 cm^{-1} describes the synthesis of the SnS pair and metal oxide stretches. As a result of the chemicals used during the synthesis process, the sample also contained additional functional groups at various peaks corresponding to CO_2, C=O, C-H and -OH etc.

Scanning Electron Micrograph (SEM) Characteristics

A field emission scanning electron microscope (FESEM) was used to assess the morphology and grain size of the synthesised nanostructure. The elemental content of the fabricated nanostructure thin film on ITO substrate was also examined using SEM-EDX that was shown in Fig. 4.

According to obtained SEM images the grain size deposited on the ITO substrate has the range 24.1 nm to 50.9 nm which was shown in Fig. 5. This obtained size of nanostructures verifies the crystal size calculated by Debye-Scherrer equation for XRD pattern.

Some information about In, Si, O was also presented in the EDX spectrum that was due to the substrate used and others were due to the chemical processed during the experiment analysis.

Using particles in the deposited nanostructures with comparable particle sizes of the order of several nanometers, Image J software was used to analyse the evaluation of grain sizes and their distribution in the composites. The deposited thin film was made up of particles with an average size of 58.9 nm and 43.43 nm with standard deviation 19.23 and 14.26 nm as shown in Fig. 6, which was obtained for the SEM micrographs shown in Fig. 4 and 5. This estimate was made from the Gaussian fitting of the particle distribution diagram as shown in Fig. 6 (a & b).

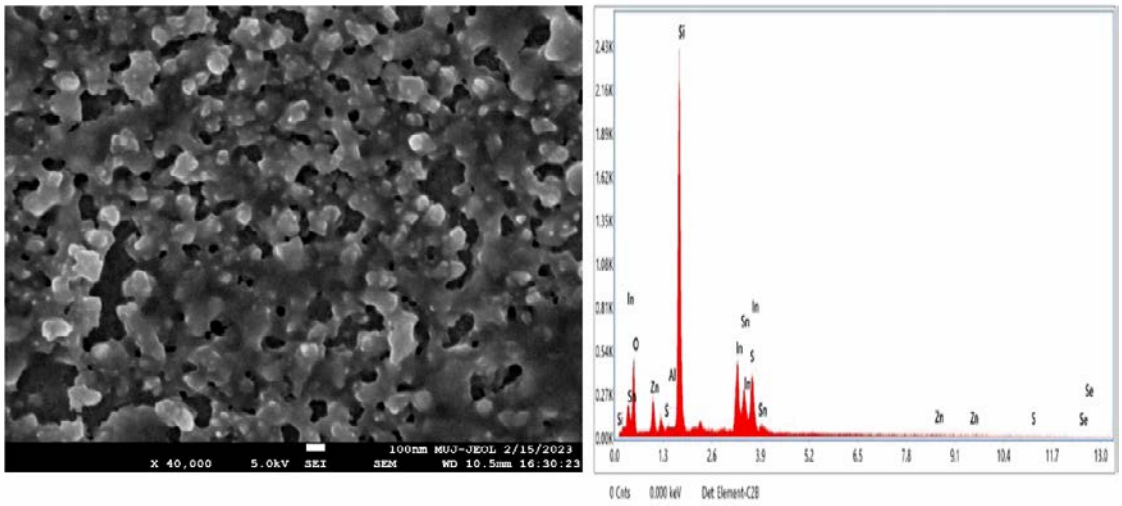

Figure 4: SEM image of deposited SnS nanostructure with elemental mapping

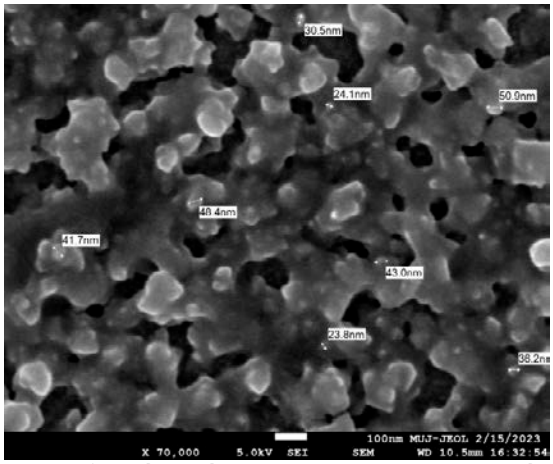

Figure 5: Synthesized SnS Nanostructure in a micrograph

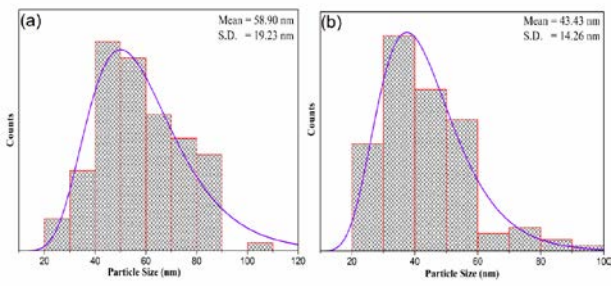

Figure 6: Particle size distribution diagram

Electrical Properties

Keithley Electrometer 6517A was used to test electrical characteristics such as current-voltage (I-V) characteristics in darkness, LED of 2.4W and normal light (tungsten filament) of 100W in the range of -2.5 volt to 2.5 volt at ambient temperature which were shown in Fig. 7. There was a remarkable change in the current for the tungsten filament light and for LED as compared to the dark mode and have similar behaviour both in forward bias and reverse bias. SnS is a direct band gap material in which the electronic configuration of Sn is [Kr] $5s^2 4d^{10} 5p^2$ and S is [Ne] $3s^2 3p^4$. The concentration of the carriers and the mobility of the charges determine the conductivity of thin films made of synthetic nanostructures. Electrical conductivity varies mostly according to the grain size deposited on nanostructure as well as the presence of other phases. It has an almost straight-line pattern, which suggests that the ITO/SnS junctions are ohmic up to 1.5V. Because its low cost, high theoretical capacity (1137 mAh/g for Li-ion batteries and 1022 mAh/g for Na-ion batteries), large interlayer spacing (0.559 nm), and low discharge potential, SnS, a typical black phosphorus analogues (BPA) material, has gained a lot of interest in energy devices [30-33]. Because of its acceptable bandgap, high absorption coefficient, and conductivity, earth abundant SnS has demonstrated remarkable features in thin-film solar cells in recent years [28,34-35]. Devika et al. (2006) studied the variation in conductivity of SnS nanostructures with temperature and reported that with increasing temperature, there is a steep variation in conductivity due to carrier excitation from the valence band to the conduction band, which is responsible for this acute difference in conductivity [4,36].

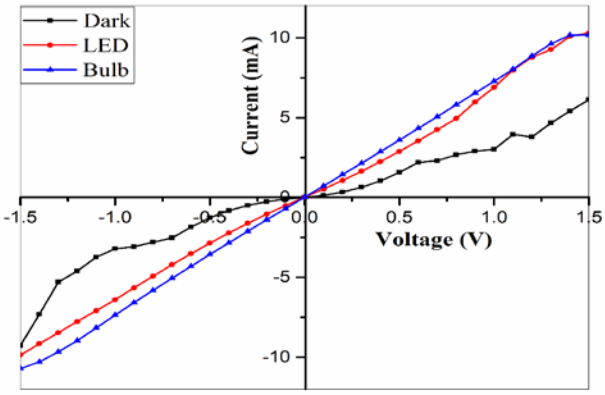

Figure 7: Current-voltage characteristics of synthesized SnS nanostructure thin film

Conclusions

SnS thin films were synthesized using an inorganic electrolyte solution and nanostructures deposited on an ITO substrate using a two-electrode cell setup. By using various characterisation techniques, the structural, optical, and electrical properties of the deposited SnS nanostructure thin film were examined. The deposited SnS thin films have an orthorhombic layered structure with a preferred (111) plane, according to XRD studies and are around the size of nanocrystalline crystals. The SEM image demonstrated the homogeneous structure and substrate stickiness of the SnS nanostructure thin films. The optical

band gap of the deposited SnS nanostructure was calculated to be 1.31 eV. The optical bandgap of the deposited film is less than that of the bulk due to the existence of defect states. The film exhibits a high proportion of visible light absorption, a low optical band gap, and good conductivity. Mahdi et al. reported that by adjusting the concentration of the complexing agent trisodium citrate during the deposition process, the phases present in tin sulphide can be adjusted [2]. Due to their excellent optoelectronic characteristics, it is suggested that SnS thin films could be used as the ideal absorber layer in solar cells. Therefore, it is essential to develop easy methods for rapidly creating high-quality and well-defined SnS based nanostructures on a wide scale that are also inexpensive and environmentally safe.

ACKNOWLEDGEMENT

The authors are thankful to Director, CNCER and Head Department of Physics, University of Rajasthan, Jaipur to provide the facility for the synthesis and characterization.

References

1. Vikraman, D., Thiagarajan, S., Karuppasamy, K., Sanmugam, A., Choi, J. H., Prasanna, K. & Kim, H. S. Shape-and size-tunable synthesis of tin sulphide thin films for energy applications by electrodeposition, Applied Surface Science, 479, 2019, 167-176.
2. Mahdi, M., Ibrahim, K., Hmood, A., Ahmed, N., & Mustafa, F. Control of Phase, Structural and Optical Properties of Tin Sulfide Nanostructured Thin Films Grown via Chemical Bath Deposition, Journal of Electronic Materials, 46(7), 2017, 1-10.
3. Ghosh, B., Roy, R., Chowdhury, S., Banerjee, P., & Das, S. Synthesis of SnS thin films via galvanostatic electrodeposition and fabrication of CdS/SnS heterostructure for photovoltaic applications, Applied surface science, 256(13), 2010, 4328-4333.
4. Devika, M., Ramakrishna Reddy, K. T., Koteeswara Reddy, N., Ramesh, K., Ganesan, R., Gopal, E. S. R., & Gunasekhar, K. R. Microstructure dependent physical properties of evaporated tin sulfide films, Journal of Applied Physics, 100(2), 2006, 023518(1-7).
5. Martin, A. G., Keith, E., Yoshihiro, H., & Wilhelm, W. Solar cell efficiency tables (Version 34), Progress in photovoltaics: research and applications, 17(5), 2009, 320-326.
6. Wadia C., Alivisatos, A. P., Kammen, D. M. Materials availability expands the opportunity for large-scale photovoltaics deployment, Environ. Sci. Technol., 43 (6), 2009, 2072–2077.
7. Zainal, Z., Hussein, M. Z., & Ghazali, A. Cathodic electrodeposition of SnS thin films from aqueous solution, Solar energy materials and solar cells, 40(4), 1996, 347-357.
8. Yue, G. H., Peng, D. L., Yan, P. X., Wang, L. S., Wang, W., & Luo, X. H. Structure and optical properties of SnS thin film prepared by pulse electrodeposition, Journal of Alloys and Compounds, 468(1-2), 2009, 254-257.
9. Ruhle, S. Tabulated values of the Shockley–Queisser limit for single junction solar cells, Solar energy, 130, 2016, 139-147.
10. Kh, A. N., Bankina, V. F., Poretskaya, L. V., Shelimova, L. E., & Skudnova, E. V. Semiconducting II–VI, IV–VI and V–VI Compounds, NY: Plenum Press, 249, 1969, 14.
11. Huang, W., Li, C., Gao, L., Zhang, Y., Wang, Y., Huang, Z. N., & Zhang, H. Emerging black phosphorus analogue nanomaterials for high-performance device applications, Journal of Materials Chemistry C, 8(4), 2020, 1172-1197.
12. Tian, Z., Guo, C., Zhao, M., Li, R., & Xue, J. Two-dimensional SnS: a phosphorene analogue with strong in-plane electronic anisotropy, ACS Nano, 11(2), 2017, 2219-2226.
13. Gomes, L. C., & Carvalho, A. Phosphorene analogues: Isoelectronic two-dimensional group-IV monochalcogenides with orthorhombic structure, Physical Review B, 92(8), 2015, 085406(1-8).
14. Ghosh, B., Das, M., Banerjee, P., & Das, S. Fabrication and optical properties of SnS thin films by SILAR method, Applied surface science, 254(20), 2008, 6436-6440.
15. Abdelrahman, A. E., Yunus, W. M. M., & Arof, A. K. Optical properties of tin sulphide (SnS) thin film estimated from transmission spectra, Journal of non-crystalline solids, 358(12-13), 2012, 1447-1451.
16. Johny, J., Sepulveda-Guzman, S., Krishnan, B., Avellaneda, D. A., Aguilar Martinez, J. A., & Shaji, S. Synthesis and properties of tin sulfide thin films from nanocolloids prepared by pulsed laser ablation in liquid, ChemPhysChem, 18(9), 2017, 1061-1068.
17. Thiruramanathan, P., Hikku, G. S., Sharma, R. K., & Shakthi, M. S. Preparation and characterization of indium doped SnS thin films for solar cell applications, Int. J. TechnoChem Res, 1(1), 2015, 59-65.
18. Reddy, K. R., Reddy, N. K., & Miles, R. W. Photovoltaic properties of SnS based solar cells, Solar energy materials and solar cells, 90(18-19), 2006, 3041-3046.
19. Leach, M., Reddy, K. R., Reddy, M. V., Tan, J. K., Jang, D. Y., & Miles, R. W. Tin sulphide thin films synthesised using a two-step process, Energy Procedia, 15, 2012, 371-378.
20. Garmim, T., Chahib, S., Soussi, L., Mghaiouini, R., Jouad, Z. E., Louardi, A., & Monkade, M. Optical, electrical and electronic properties of SnS thin films deposited by sol gel spin coating technique for photovoltaic applications, Journal of Materials Science: Materials in Electronics, 31, 2020, 20730-20741.
21. Avellaneda, D., Nair, M. T. S., & Nair, P. K. Polymorphic tin sulphide thin films of zinc blende and orthorhombic structures by chemical deposition, Journal of the Electrochemical Society, 155(7), 2008, D517-D525.
22. Sinsermsuksakul, P., Heo, J., Noh, W., Hock, A. S., & Gordon, R. G. Atomic layer deposition of tin monosulfide thin films, Advanced Energy Materials, 1(6), 2011, 1116-1125.
23. Arepalli, V. K., Dai Nguyen, T., & Kim, J. Influence of Ag thickness on the structural, optical, and electrical properties of the SnS/Ag/SnS trilayer films for solar cell application, Current Applied Physics, 20(3),2020, 438-444.
24. Steichen, M., Djemour, R., Gütay, L., Guillot, J., Siebentritt, S., & Dale, P. J. Direct synthesis of single-phase p-type SnS by electrodeposition from a dicyanamide ionic liquid at high temperature for thin film solar cells, The Journal of Physical Chemistry C, 117(9), 2013, 4383-4393.
25. Cheng, S., He, Y., & Chen, G. Structure and properties of SnS films prepared by electro-deposition in presence of EDTA, Materials Chemistry and Physics, 110(2-3), 2008, 449-453.
26. Patel, M., Mukhopadhyay, I., & Ray, A. Annealing influence over structural and optical properties of sprayed SnS thin films, Optical materials, 35(9), 2013, 1693-1699.
27. Tauc J., Grigorovici R. & Vancu A., Optical Properties and Electronic Structure of Amorphous Germanium, Basic Solid-State Physics 15, 1966, 627–637.
28. Huang, W., Xie, Z., Fan, T., Li, J., Wang, Y., Wu, L., & Zhang, H. Black-phosphorus-analogue tin monosulfide: an emerging optoelectronic two-dimensional material for high-performance photodetection with improved stability under ambient/harsh conditions, Journal of Materials Chemistry C, 6(36), 2018, 9582-9593.
29. Abdullah, B.J., Size effect of band gap in semiconductor nanocrystals and nanostructures from density functional theory within HSE06. *Materials Science in Semiconductor Processing*, 137, 2022, 106214.
30. Wei, Z., Wang, L., Zhuo, M., Ni, W., Wang, H., & Ma, J. Layered tin sulfide and selenide anode materials for Li-and Na-ion batteries, Journal of Materials Chemistry A, 6(26), 2018, 12185-12214.
31. Shan, Y., Li, Y., & Pang, H. Applications of tin sulphide-based materials in lithium-ion batteries and sodium-ion batteries, Advanced Functional Materials, 30(23),2020, 2001298(1-31).
32. Xia, J., Liu, L., Jamil, S., Xie, J., Yan, H., Yuan, Y., & Cao, G. Free-standing SnS/C nanofiber anodes for ultralong cycle-life

lithium-ion batteries and sodium-ion batteries, Energy Storage Materials, 17, 2019, 1-11.

33. Choi, S. H., & Kang, Y. C. Aerosol-assisted rapid synthesis of SnS-C composite microspheres as anode material for Na-ion batteries, Nano Research, 8, 2015, 1595-1603.
34. Huang, W., Li, C., Gao, L., Zhang, Y., Wang, Y., Huang, Z. N., & Zhang, H. Emerging black phosphorus analogue nanomaterials for high-performance device applications, Journal of Materials Chemistry C, 8(4), 2020, 1172-1197.
35. Le Donne, A., Trifiletti, V., & Binetti, S. New earth-abundant thin film solar cells based on chalcogenides, Frontiers in chemistry, 7, 2019, 297(1-13).
36. Johny, J., Sepulveda-Guzman, S., Krishnan, B., Avellaneda, D. A., Martinez, J. A., Anantharaman, M. R., & Shaji, S. Tin sulfide: Reduced graphene oxide nanocomposites for photovoltaic and electrochemical applications, Solar Energy Materials and Solar Cells, 189, 2019, 53-62.